Brain Tumor Pathology (2019) 36:152–161
https://doi.org/10.1007/s10014-019-00350-1

ORIGINAL ARTICLE

Clinicopathological evaluation of PD-L1 expression and cytotoxic T-lymphocyte infiltrates across intracranial molecular subgroups of ependymomas: are these tumors potential candidates for immune check-point blockade?

Aruna Nambirajan[1] · Prit Benny Malgulwar[1] · Agrima Sharma[1] · Meher Thej Boorgula[2] · Ramesh Doddamani[2] · Manmohan Singh[2] · Vaishali Suri[1] · Chitra Sarkar[1] · Mehar Chand Sharma[1]

Received: 21 May 2019 / Accepted: 25 July 2019 / Published online: 6 August 2019

Abstract

Immune check-point blockade (ICB) targeting programmed cell death ligand-1 (PD-L1)/programmed death-1 (PD-1) axis has created paradigm shift in cancer treatment. 'ST-RELA' and 'PF-A' molecular subgroups of ependymomas (EPN) show poor outcomes. We aimed to understand the potential candidature of EPNs for ICB. Supratentorial (ST) Grade II/III EPNs were classified into ST-RELA, ST-YAP, and ST-not otherwise specified (NOS), based on *RELA/YAP1* fusion transcripts and/or L1CAM and p65 protein expression. Posterior fossa (PF) EPNs were classified into PF-A and PF-B based on H3K27me3 expression. Immunohistochemistry for PD-L1 and CD8 was performed. RelA protein enrichment at *PDL1* promoter site was analysed by chromatin immunoprecipitation-qPCR (ChIP-qPCR). Eighty-three intracranial EPNs were studied. Median tumor infiltrating CD8 + cytotoxic T-lymphocyte (CTL) density was 6/mm^2, and was higher in ST-EPNs (median 10/mm^2) as compared to PF-EPNs (median 3/mm^2). PD-L1 expression was noted in 17/83 (20%) EPNs, including 12/31 ST-RELA and rare ST-NOS (2/12), PF-A (2/25) and PF-B (1/13) EPNs. Twelve EPNs (14%) showed high CTL density and concurrent PD-L1 positivity, of which majority (10/12) were ST-RELA EPNs. Enrichment of RelA protein was seen at *PDL1* promoter. Increased CTL densities and upregulation of PD-L1 in ST-RELA ependymomas suggests potential candidature for immunotherapy.

Keywords Ependymoma · Intracranial · Lymphocytes · CD8 · PD-L1 · NF-KB

Introduction

Ependymomas (EPNs) are relatively circumscribed gliomas that recapitulate the light microscopic and ultrastructural features of ependymal cells lining the ventricles and central canal of the spinal cord [1]. They show site-specific differences in their demographic profile, molecular alterations and biological behaviour, and WHO histological grade, by itself, is of limited prognostic value [2]. Recent DNA methylation profiling studies have identified nine molecular subgroups, three in each major anatomical compartment: supratentorium (ST), posterior fossa (PF) and spinal cord [3]. ST Grade II/III EPNs harboring fusions of *RELA* (v-rel avian reticuloendotheliosis viral oncogene homolog A) [4] and PF Grade II/III EPNs with a CpG-island methylator phenotype [5] constitute the ST-RELA and PF-A molecular subgroups, respectively [3].

Part of this study has been presented at the 19th International Congress of Neuropathology held at Tokyo, Japan in September, 2018 and published as an abstract.

Aruna Nambirajan and Prit Benny Malgulwar are co-first authors.

Electronic supplementary material The online version of this article (https://doi.org/10.1007/s10014-019-00350-1) contains supplementary material, which is available to authorized users.

✉ Mehar Chand Sharma
sharmamehar@yahoo.co.in

[1] Department of Pathology, All India Institute of Medical Sciences, Ansari Nagar, New Delhi 110029, India

[2] Department of Neurosurgery, All India Institute of Medical Sciences, New Delhi 110029, India

They account for more than 2/3rd of all intracranial EPNs, predominate in children and are associated with extremely poor 5-year overall (~ 50%) and progression-free (~ 20%) survival rates [3]. Expression of proteins L1CAM and p65/RelA [4, 6, 7] and loss of H3K27me3 [8] have been proposed as surrogate markers for ST-RELA and PF-A subgroups, respectively. However, viable therapeutic protocols tailored to benefit these patients are yet to be developed [2].

Genomic instability is the hallmark of cancer. With increasing random mutations occurring in tumor cells, neoantigens capable of being recognised as 'foreign' by host immune cells are being created. One of the mechanisms by which tumor cells escape such immune surveillance is by upregulating physiological immune check points such as programmed death-ligand 1 (PD-L1/CD274) on their surface, which by means of engagement with programmed death-1 (PD-1) receptors on infiltrating cytotoxic T-lymphocytes (CTLs) lead to T-cell exhaustion [9]. Immune checkpoint blockade (ICB) using monoclonal antibodies against PD-L1/PD-1 interrupts these interactions, reactivates CTLs, and leads to tumor cell elimination. Such therapy has been found to produce prolonged clinical remissions in subsets of patients with advanced solid organ malignancies [9]. Among brain tumors, many clinical trials using ICB are on-going in patients with brain metastases and glioblastoma [10]. Limited studies on the expression of PD-L1 and its immune correlates in EPNs have revealed contradictory results [11–16]. With the aim of understanding the potential candidature of EPNs for ICB, we performed this study to analyse the expression of PD-L1 in a large cohort of intracranial EPNs in correlation with molecular subgroups and CTL infiltrates.

Materials and methods

The study was of retrospective design spanning thirteen years (2003–2016) duly approved by the institute ethics committee (Ref No: IEC-602/03.11.2017). Informed consent was waived in view of retrospective nature of the study.

Case selection

All intracranial EPNs with adequate tumor tissue in the formalin-fixed paraffin-embedded (FFPE) blocks were retrieved from the archives and diagnosis reconfirmed by two independent pathologists (AN, MCS) according to the latest WHO classification of CNS tumors [1]. All immunohistochemistry (IHC) was performed on FFPE whole-tumor sections on the Ventana BenchMark XT.

Molecular subgrouping of intracranial ependymomas

In ST Grade II/III EPNs, Quantitative Real-time PCR (qRT-PCR) for type 1 and 2 C*11orf95-RELA* fusion transcripts, and *YAP1-MAMLD1* and *YAP1-FAM118B* fusion transcripts was performed as previously described [6]. Membranous staining in > 50% of tumor cells was interpreted positive for L1CAM (Sigma, Germany, 1:100 dilution) [7]. Nuclear staining in > 50% tumor cells was interpreted positive for p65 (Spring Biosciences, USA, 1:400 dilution) [7]. ST EPNs harboring type 1 and/or 2 *C11orf95-RELA* fusion transcripts were categorized as ST-RELA. Among supratentorial ependymomas lacking type 1 and 2 fusion transcripts, those showing unequivocal tumor cell staining for both L1CAM and p65 proteins were also categorized as ST-RELA [7]. Ependymomas with *YAP1* fusions were categorized as ST-YAP, and the remaining were categorized as 'Not otherwise specified' (ST-NOS).

PF EPNs with diffuse loss of H3K27me3 expression (1:200, C36B11, Cell signaling Technology) in tumor cells were classified as PF-A [8], while the remaining were classified as PF-B. Grade I subependymomas (SE) were classified based on their site into ST-SE or PF-SE (Supplementary Fig. 1).

Quantification of CD8 + cytotoxic T-lymphocytes (CTLs)

Following IHC for CD8 (DBS, 1:50), whole tumor sections were scanned on low power magnification and 3 hot-spots were photographed at 200 × magnification. CD8 + CTLs infiltrating between tumor cells were manually tagged and counted on image analysis software (Image ProPlus Version 7, Media Cybernetics) to obtain tumor-infiltrating CTL density/mm^2. Intra-vascular CTLs, perivascular CTLs and CTLs in areas corresponding to one high-power (40 × objective) magnification field around zones of necrosis were excluded during counting (Supplementary Fig. 2).

Perivascular CTLs (PVC) were noted separately in at least 10 vascular channels in hotspots and graded as follows: sparse PVC—mean perivascular CTL density of 0–5 CTLs/vessel; dense PVC—mean perivascular CTL density > 5 CTLs/vessel.

Tumor margin was assessed wherever sampled and graded as follows: 0—no CTLs, 1—scattered CTLs, and 2—band-like CTL infiltrates.

PD-L1 immunohistochemistry

PD-L1 IHC was performed using SP263 clone (pre-diluted, Ventana, USA). PD-L1 tumor proportion score (TPS) was calculated as a percentage of total tumor component showing focal/complete membranous ± cytoplasmic staining of any intensity. Expression in ≥ 1% of tumor cells was considered positive [17].

Chromatin immunoprecipitation-quantitative polymerase chain reaction

Chromatin immunoprecipitation-qPCR (ChIP-qPCR) was performed on 3 fresh ST-RELA samples. Briefly, fresh frozen EPN tumor samples were thawed on ice, chopped into small pieces, and cross-linked in 1% formaldehyde in PBS for 10 min. The crosslinking reaction was stopped using 100 µl of 125 mM glycine. The chromatin was fragmented using Diagenode Bioruptor plus at high power settings (as per manufacturers' guidelines). Fragmented chromatin was immunoprecipitated using RelA (M/s Santacruz Biotechnology) and IgG (M/s Abcam) antibodies as per Low cell ChIP kit guidelines (M/s Diagenode). After overnight incubation, immunoprecipitated and input DNAs were purified in 40 µl of water with IPure kit following the manufacturer's instructions (M/s Diagenode). qPCRs were performed on 2 µl of DNA in a LC480 system (Roche) using Syber green dye for PDL1/CD274 promoter site and GAPDH. The sequences of the primers used for detection are provided in Supplementary Table 1. Enrichment was expressed as the percent input using the following formula: % of total input = $100 \times 2^{[Ct (ChIP) - (Ct input - log2 (input dilution factor)]}$.

Statistical analysis

All statistical analyses were performed using GraphPad Prism Version 8 (GraphPad Software Inc., San Diego, CA). Associations among clinicopathological factors were tested using Fisher's exact test or non-parametric *t* test (Mann–Whitney test). The correlation between PD-L1 TPS and CTL density was calculated using the Spearman correlation test. Survival analysis was performed using the Kaplan–Meier method and the log-rank test. All statistical tests were 2-sided and $p < 0.05$ was considered statistically significant.

Results

Clinicopathological features

A total of 83 intracranial ependymomas from 81 patients were included (Fig. 1). Additional samples obtained from tumor recurrences were available in 2 patients (patient I.D. 21 and 22). Median patient age at diagnosis was 9 years (range 1–62 years). Male: female ratio was 1.6:1. Predominant tumors were of WHO histological grade III (71%, 52/83) followed by grade II (36%, 30/83).

On molecular subgrouping, ST-RELA ($n = 31$) and PF-A ($n = 25$) constituted the majority subgroups. Eighteen ST EPNs harboured type 1 and/or 2 *C11orf95-RELA* fusion transcripts, of which all were immunopositive for L1CAM (18/18, 100%) and 14/18 (78%) were immunopositive for p65. RT-PCR failed in 5 cases while type 1 or 2 *RELA* fusions were not detected in the remaining ST EPNs. Thirteen of the ST EPNs with negative/failed RT-PCR results showed dual immunopositivity for L1CAM and p65. Previous validation studies have demonstrated that dual immunopositivity for L1CAM and p65 has a high positive predictive value for presence of *RELA* fusions [7] and these cases may harbour alternate/variant *RELA* fusion transcripts that cannot be detected by our primer design [6]. Therefore, these cases were also categorized as ST-RELA EPNs. One tumor harboured *YAP1-MAMLD1* fusion transcript and was categorized as ST-YAP. The remaining ST EPNs including one with isolated L1CAM positivity and two with isolated p65 staining were classified as ST-NOS (Fig. 1, Supplementary Fig. 1).

ST-RELA and PF-A subgroups predominated in children with grade III preponderance. Majority of tumor samples were primary ependymomas (68/83). Fifteen recurrent EPN samples included were represented among the ST-RELA (10/31), ST-NOS (3/12), PF-A (1/25) and PF-B (1/13) subgroups. Only four patients with recurrent ST-RELA tumors (patient I.D.s 22, 24, 27, 29) had records of receiving radiotherapy (RT) following resection of primary. One patient (patient I.D. 23) had not received RT, while treatment history could not be retrieved in the others (Fig. 1).

Follow-up was available in 56 patients (68%) with a median follow-up duration of 18 months (range 3–113 months) post-resection. At the time of completion of this study (February 2019), eighteen patients were alive with tumor recurrence while eight patients had died of tumor-related complications. Six patients died in the perioperative period (during and within 4 weeks of surgery), while the remaining were alive without any evidence of tumor recurrence. All 26 patients experiencing progressive events (recurrence/death) had undergone a gross total resection. Majority of their primary tumors belonged to ST-RELA (11/26, 42%) and PF-A (9/26, 35%) subgroup (Fig. 1). Details of adjuvant radiotherapy/chemotherapy were not available. On progression-free survival (PFS) analysis of patients presenting with primary ependymomas (patients with recurrent ependymomas were excluded from all survival analysis), PF-B ependymomas showed longer PFS as compared to the ST-RELA, ST-NOS, and PF-A

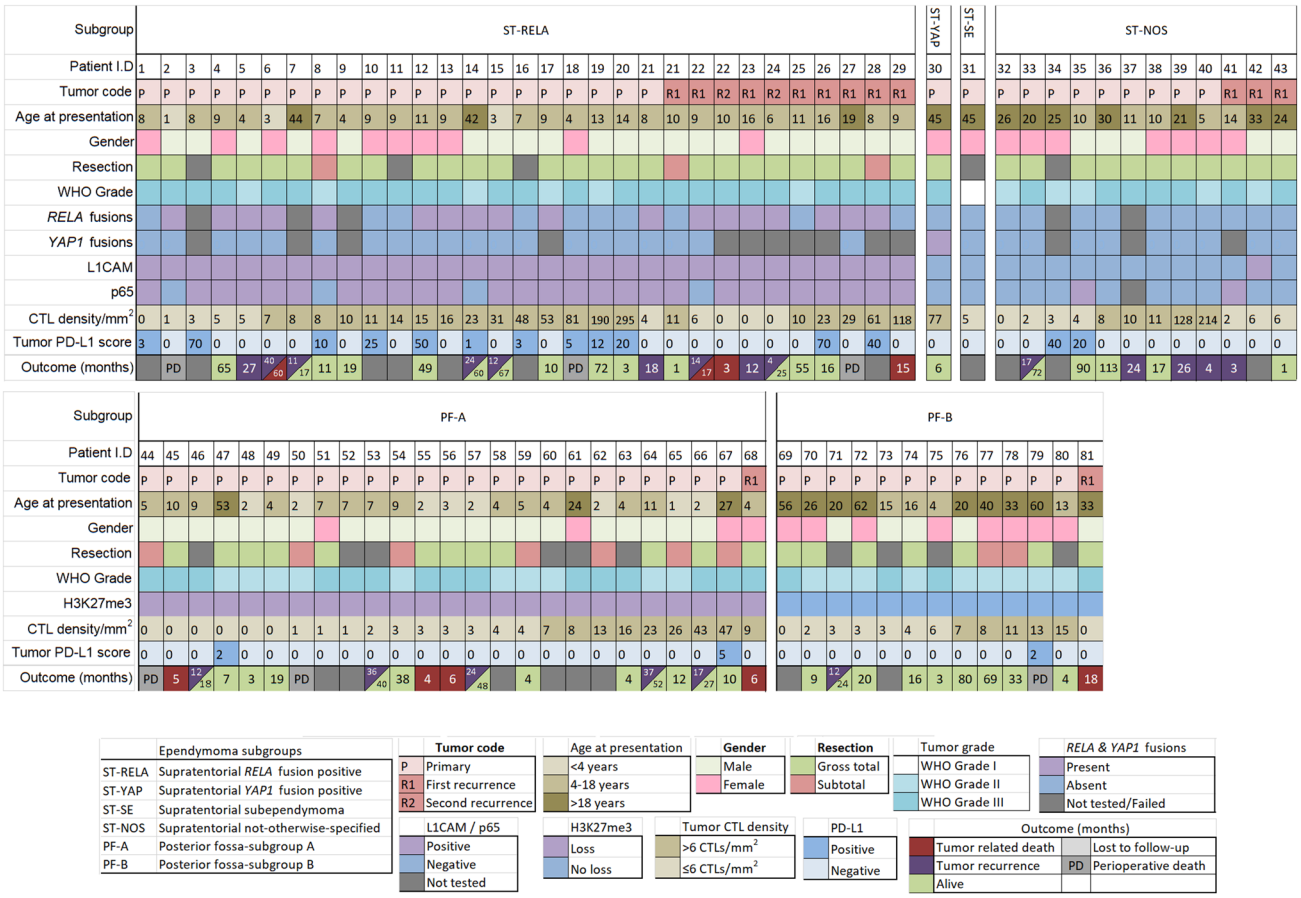

Fig. 1 Clinicopathological features of intracranial ependymomas included in the study

(Supplementary Fig. 1G), although this did not reach statistical significance ($p = 0.33$). Multivariate and overall survival analysis were not done due to relatively small number of deaths.

Cytotoxic T-cell infiltrates

The median tumor-infiltrating CTL density among all intracranial EPNs was 6 CTLs/mm^2, ranging from 0 to up to 295 CTLs/mm^2, and was significantly higher among ST EPNs (10 CTLs/mm^2, range 0–295) as compared to PF EPNs (3 CTLs/mm^2, range 0–47) ($p = 0.003$) (Table 1). Among molecular subgroups, the intra-tumoral CTL densities were significantly higher in ST-RELA as compared to PF-A and PF-B EPNs while the differences did not reach statistical significance among the others (Fig. 2a). Highest median CTL densities were seen in ST-RELA tumors followed by ST-NOS with no significant difference in CTL densities between primary and recurrent tumor samples of ST-RELA ($p = 0.6$) or ST-NOS ($p = 0.5$) (Table 1). Even among the two paired patient samples available (i.e., patient ID 21 and 22 in Fig. 1), there was no significant increase or decrease in CTL densities in the recurrence. There was no significant correlation of CTL densities with age, gender or WHO grade (Fig. 1).

Dense perivascular infiltrates were seen in 17% (14/83) EPNs, belonging to the ST-RELA (7/31), ST-YAP (1/1), ST-NOS (4/12) and PF-B (2/13) subgroups (Fig. 2b). Although primary ST-RELA and ST-NOS more frequently harboured dense perivascular infiltrates than recurrent samples, the difference did not reach statistical significance ($p > 0.5$) (Table 1). Presence of dense perivascular infiltrates significantly correlated with a higher tumor-infiltrating CTL density ($p = 0.004$) (Fig. 2c).

Tumor margin was sampled in 21 cases, most of which lacked any significant inflammation. Sparse scattered CTLs were seen in 3 cases of ST-RELA (patient IDs: 3, 16, 26 in Fig. 1) and a band-like infiltrate was seen in a single ST-NOS (patient ID: 40 in Fig. 1) (Fig. 2d).

Tumor infiltrating CTL density > 6/mm^2 correlated with a longer PFS (median PFS of 37 months vs. 24 months) among all primary EPNs although this did not reach statistical significance ($p = 0.2$) (Fig. 2e). Among primary ST-RELA samples, those with CTL densities > 6/

Table 1 Density of cytotoxic T-lymphocytes and PD-L1 protein expression in intracranial molecular subgroups of ependymomas

Subgroup	No. of samples	Median tumor-infiltrating CTLs/mm^2 (range)	Dense perivascular CTL infiltrates *n* (%)	PD-L1 protein expression in ≥ 1% tumor cells *n* (%)	Spearmen correlation co-efficient between PD-L1 tumor proportion score and tumor-infiltrating CTL density/mm^2 (95% confidence intervals with *p* value)
All ependymomas	83	6 (0–295)	14 (17)	17 (20)	0.26 (0.04–0.45, 0.01)
ST-RELA					
All	31	11 (0–295)	7 (23)	12 (39)	0.34 (− 0.03 to 0.6, 0.06)
Primary	21	11 (0–295)	7 (33)	10 (48)	0.24 (− 0.23 to 0.61, 0.3)
Recurrent	10	10.5 (0–118)	0 (0)	2 (20)	0.42 (NA to NA, 0.2)
ST-NOS					
All	12	6 (0–214)	4 (33)	2 (18)	− 0.26 (− 0.73 to 0.38, 0.4)
Primary	9	8 (0–214)	3 (33)	2 (22)	− 0.32 (NA to NA, 0.4)
Recurrent	3	6 (2–6)	1 (33)	0 (0)	0
ST-YAP1					
Primary	1	77	1 (1)	0 (0)	NA
ST-SE					
Primary	1	5	0 (0)	0 (0)	NA
PF-A					
All	25	3 (0–47)	0 (0)	2 (8)	0.07 (− 0.34 to 0.46, 0.7)
Recurrent	1	9	0	0	NA
PF-B					
All	13	4 (0–15)	2 (8)	1 (7)	0.39 (− 0.22 to 0.78, 0.3)
Recurrent	1	0	0	0	NA

PD-L1 programmed death ligand 1, *ST* supratentorial, *NOS* not otherwise specified, *SE* subependymoma, *PF* posterior fossa, *CTL* cytotoxic T-lymphocytes, *NA* not applicable

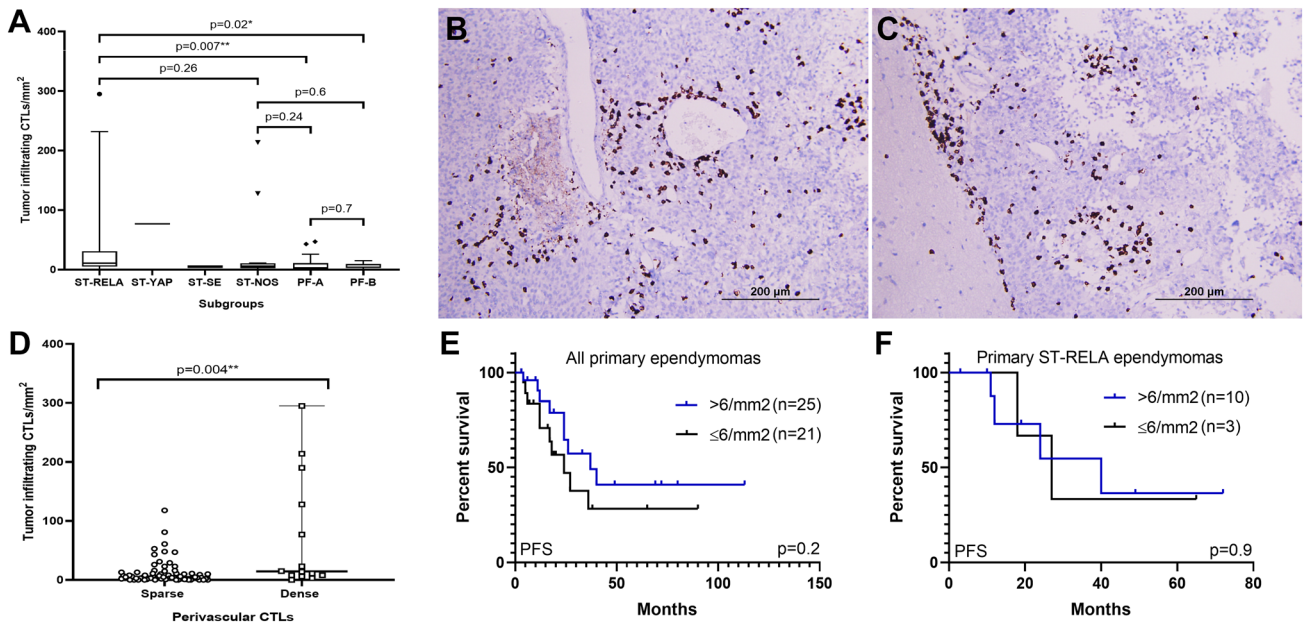

Fig. 2 Cytotoxic T-lymphocyte infiltrates in intracranial ependymomas. **a** Box and whisker plot for tumor-infiltrating cytotoxic T-lymphocyte numbers/mm^2 across the molecular subgroups of intracranial ependymomas. Whiskers represent 5 and 95% confidence intervals. Representative microphotographs of an ST-NOS ependymoma showing CD8 + cytotoxic T-lymphocytes in perivascular locations (**b**) and along the brain–tumor interface (**c**). **d** Presence of dense perivascular CD8 + cytotoxic T-lymphocytes correlates with higher tumor-infiltrating CTL density. Correlation of high CD8 + cytotoxic T-lymphocyte density with progression-free survival among all primary ependymomas (**e**) and among the ST-RELA tumors (**f**)

mm^2 associated with longer median PFS of 40 months vs. 27 months in those with low CTL densities, however, this difference also did not reach statistical significance (Fig. 2f).

PD-L1 protein expression

PD-L1 protein expression in ≥ 1% of tumor cells was seen in 20% of all EPNs, predominantly belonging to the ST-RELA subgroup (39%) and including small numbers of ST-NOS, PF-A, and PF-B EPNs (Table 1, Figs. 1, 3a, b). It was more frequently positive in primary ST-RELA (48%) as compared to recurrent ST-RELA samples (20%) ($p > 0.5$), while it was not expressed in recurrent samples of other subgroups (Table 1). Among the 2 paired patient samples available, all four were PD-L1-negative (Fig. 1). PD-L1-positive primary EPNs (Fig. 2d) showed a trend towards longer PFS (median PFS not reached) as compared to PD-L1-negative cases (median PFS 26 months) ($p > 0.5$) and a similar trend was seen among the primary ST-RELA subset as well (Fig. 2e).

PD-L1 was also expressed in tumor-associated myeloid cells in 7% of all EPNs (6/83), consisting of 4 ST-RELA and 2 ST-NOS cases (Fig. 3c).

There was no significant correlation of PD-L1 expression with age, gender or WHO grade (Fig. 1).

Correlation of intra-tumoral CTL density with PD-L1 protein expression

The proportion of tumor cells expressing PD-L1 significantly correlated with increasing density of tumor-infiltrating CTL density/mm^2 in all EPNs (Spearman correlation co-efficient $r = 0.26$, $p = 0.01$). Similar positive correlation co-efficients were also obtained among individual subsets of ST-RELA, PF-A and PF-B EPNs while a negative correlation co-efficient was found in ST-NOS samples (Table 1, Fig. 4a). The positive correlations between PD-L1 TPS and intra-tumoral CTL density were similar among primary and recurrent samples of ST-RELA (Table 1).

Using the median CTL density of 6/mm^2 as the cutoff, we divided EPNs into four immune groups: Group A—PD-L1-positive (TPS ≥ 1%) tumors with high CTL density (> 6 CTLs/mm^2) that are most likely to respond to PD-L1 blockade, Group B—PD-L1-negative tumors with high CTL density that are immunogenic but may be using alternate mechanisms of immune evasion and may not respond to PD-L1 blockade, Group C—PD-L1-negative tumors with low CTL density (≤ 6 CTLs/mm^2) that are non-immunogenic and unlikely candidates for immunotherapy, and Group D—PD-L1-positive tumors with low CTL density that likely exhibiting oncogenic upregulation of PD-L1 [18]. Majority of EPNs (44.5%, 37/83) belonged to immune Group C followed by 35.5% (29/83) belonging to immune Group B. Only 14% (12/83) of all EPNs with both high CTL densities

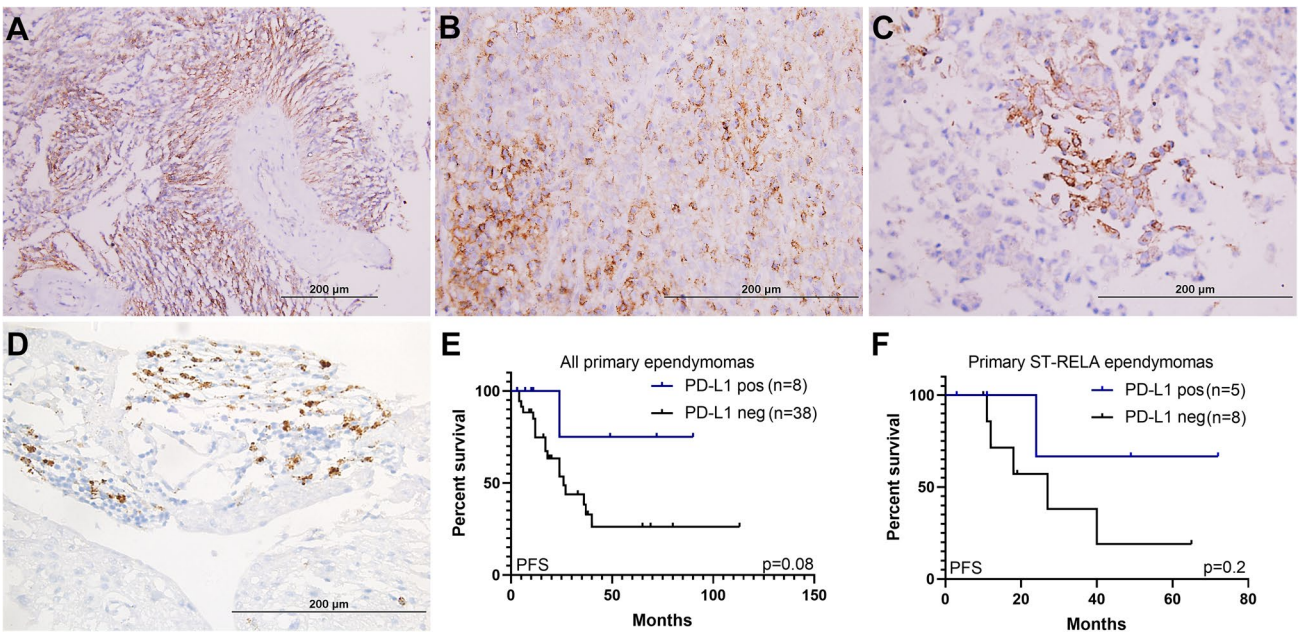

Fig. 3 PD-L1 immunohistochemistry in intracranial ependymomas. Representative microphotographs of ST-RELA (**a**, **b**) and PF-A (**c**) ependymoma showing membranous staining of tumor cells for anti-PD-L1 IHC. **d** PD-L1 expressed in tumor-associated myeloid cells in a case of ST-RELA. Correlation of PD-L1 positivity with progression-free survival among all primary ependymomas (**e**) and among the ST-RELA tumors (**f**)

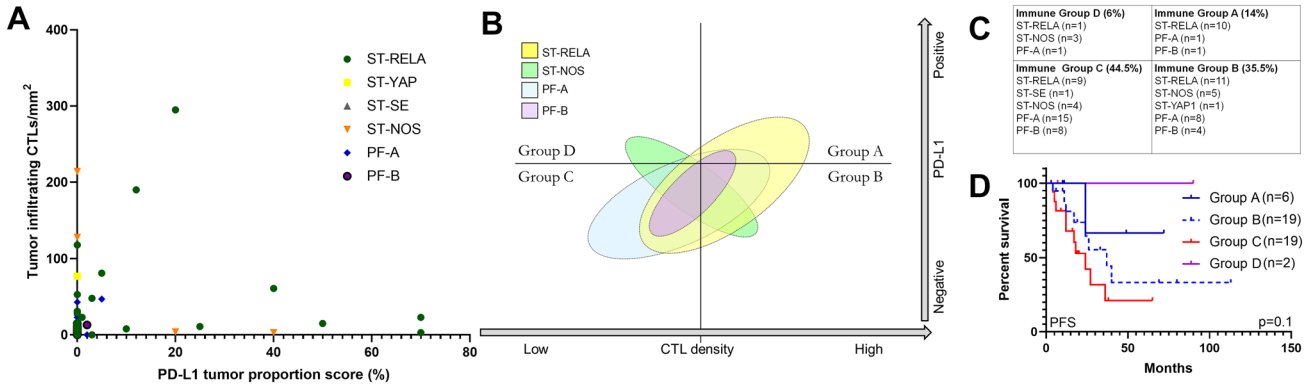

Fig. 4 Cytotoxic T-lymphocytes and PD-L1 expression across molecular subgroups of intracranial ependymomas. **a** Scatter plot showing the correlation between the proportion of tumor cells positive for PD-L1 (*x*-axis) and the tumor-infiltrating cytotoxic T-lymphocyte density/mm^2 (*y*-axis) in the six molecular subgroups. Distribution of the six molecular subgroups of ependymomas within the four immune groups (**b**, representational image; **c**, table). **d** Kaplan–Meier survival estimates show that Group C tumors show the shortest progression-free survival

and PD-L1 positivity belonged to immune Group A, while a small proportion of 6% (5/83) of cases that expressed PD-L1 in the absence of high CTL densities fell within immune Group D. Among the molecular subgroups, ~ 2/3rd of ST-RELA (68%, 21/31) showed high CTL densities, half of which were also PD-L1-positive (10/21), thus were distributed near equally within Group A and B. While the single ST-YAP ependymoma fell in immune Group B, the majority of the PF-A (60%, 15/25), PF-B (61%, 8/13), and the single ST-SE fell in Group C. ST-NOS were distributed near equally among Group B, Group C, and Group D (Fig. 4b, c). Among the four immune subgroups, primary EPNs falling in Group C showed the shortest PFS (median PFS 24 months) (Fig. 4d). We were unable to further analyse prognostic value of immune groups within molecular subgroups due to limited patient numbers.

Chromatin immunoprecipitation-quantitative polymerase chain reaction

Integrating ENCODE-Transcription Factor ChIP-seq data identified presence of RelA on *PDL1/CD274* promoter (Supplementary Fig. 3A). ChIP-qPCR on the three ST-RELA tumor samples validated presence of RelA on PDL1/CD274 promoter. The controls IgG and GAPDH were not enriched in the RelA pull down (Supplementary Fig. 3B).

Discussion

With the success of ICB in various solid organ malignancies, the potential candidature of brain tumors for ICB is now being actively explored [10]. Quantification of PD-L1 expression on tumor cells by IHC is widely being used as a predictive biomarker for ICB response [17], although its positive predictive value for ICB response is less than 33% [19]. A recent clinical trial reported lack of response to ICB in a small cohort of recurrent GBMs despite PD-L1 expression and attributed the failure to the scarcity of intra-tumoral T-lymphocytes [20]. Notably, PD-L1 expression can also occur as a result of oncogenic signalling unrelated to immune evasion and such tumors may not respond to ICB [18]. Adaptive upregulation of PD-L1 as an immune escape mechanism is usually seen in tumors with increased CTL infiltrates [21] and thus, we used a simplistic approach of immunohistochemistry for CD8 and PD-L1 to identify whether EPNs are potential candidates for immunotherapy, and ICB in particular. In our relatively large cohort of 83 intracranial EPNs and using the clinically validated SP263 PD-L1 clone, we found PD-L1 expression in 20% of all intracranial EPNs significantly correlating with increasing CTL density indicative of an adaptive immune evasion response. The majority of the PD-L1-positive EPNs belonged to the ST-RELA subgroup, the latter also encompassing tumors with the densest CTL infiltrates. Our findings are concordant with previous studies by Witt et al. and Nam et al. who reported PD-L1 protein expression in 100% (4/4) and 40% (7/15) of ST-RELA EPNs, respectively [14, 16]. These two studies also noted relatively higher numbers of T-lymphocytes in ST-RELA as compared to other EPNs [14, 16]. Witt et al. further demonstrated that the tumor-infiltrating T-lymphocytes in ST-RELA express PD-1 and are functionally exhausted [14], while Nam et al. found that the tumor-associated microglia/macrophages in ST-RELA is skewed towards the immunosuppressive M2-phenotype [16]. These observations together offer strong circumstantial evidence that ST-RELA EPNs are immunogenic, are exploiting PD-1/PD-L1

immune check points for immune evasion, and thereby are potential candidates for ICB.

One of the primary factors that determine immune recognition of tumors is their neoantigen load, as estimated by the tumor mutation burden (TMB), i.e., the total number of somatic non-synonymous mutations occurring in tumor cells [22]. Unlike adult-onset malignancies that generally arise due to gradual accumulation of random mutations over years [23], most pediatric neoplasms occur due to single driver genetic alterations and their TMB is usually low, including pediatric PF EPNs [5]. ST-RELA EPNs appear to be an exception and a number of factors, as discussed below, may be contributing to its increased immune recognition. Foremost of these, chromothripsis or random chromosomal shattering of chromosome 11 is the hallmark of ST-RELA EPNs [4] and this may contribute to increased genomic instability, neo-epitope load, and immunogenicity as has been observed in osteosarcomas [24]. While TMB estimation has not been done in a substantial number of ST EPNs, a recent clinical trial reported a very low TMB of 1.2 mutations/Mb in a PD-L1-negative pediatric ST EPN (*RELA* status not known) using a next-generation sequencing (NGS)-based assay [25]. One must bear in mind that the neoantigens in tumors undergoing chromothripsis are derived from complex chromosomal rearrangements [26] rather than due to non-synonymous mutations, and NGS techniques primarily designed to detect nucleotide substitutions are likely to underestimate the overall burden of genetic alterations in these tumors [23]. Second, loss of DNA damage repair genes, particularly *TP53*, increases tolerance to DNA damage and has been associated with higher mutation burden [22]. P53 protein accumulation indicative of functional loss of *TP53* has been commonly observed in ST-RELA EPNs [6]. Lastly, our findings indicate that tumor-infiltrating CTLs in EPNs migrate from intra-tumoral vessels rather than from the tumor margin or adjacent normal brain parenchyma. The increased microvascular densities and delicate thin-walled capillaries observed in ST-RELA EPNs may contribute to the better access of circulating immune cells to tumor neoantigens [6].

While the increased CTL infiltrates strongly favour adaptive immune upregulation of PD-L1 in ST-RELA, the role of oncogenic signalling cannot be ruled out. The wild-type *RELA* gene encodes for RelA/p56 protein, a subunit of nuclear factor-Kappa B. *RELA* fusion-encoded RelA/p65 translocates to the nucleus even at low levels resulting in constitutive NF-kB signalling [4]. NF-kB is a known regulator of *PDL1*, and functional studies show that NF-kB activation is necessary for *PDL1* upregulation following interferon-gamma release by T-lymphocytes [27–29]. Witt et al., however, noted that the tumor-infiltrating T-lymphocytes in ST-RELA failed to release interferon-gamma on stimulation [14]. Further, NF-KB activation can also be induced by epithelial to mesenchymal transition (EMT) [29], the latter known to be a key feature of ST-RELA EPNs [30]. EMT can also lead to TGF-beta-induced demethylation of the *PDL1* promoter and resultant PD-L1 upregulation [29]. While our novel ChIP experiment did demonstrate direct interaction of RelA protein with *PDL1* promoter in ST-RELA EPNs, whether the NF-KB-mediated PD-L1 upregulation in ST-RELA is a result of immune evasion or oncogenic upregulation or a combination of both needs to be clarified by functional studies and this comprehension is highly relevant for understanding how these tumors may respond to ICB.

The PF EPNs in our cohort harboured lower numbers of CTLs relative to ST EPNs, with PF-A being the most CTL-excluded molecular subgroup among all Grade II/III intracranial EPNs, in concordance with previous few studies [14, 16, 31–34]. PF-A EPNs show balanced genomes while large-scale copy number variations are characteristic of PF-B EPNs [5]. Nevertheless, both lack recurrent mutations and harbour very low TMB levels [5]. Hoffmann et al. reported that the predominant gene ontologies that distinguished the aggressive PF-A from PF-B were immune-related: PF-A was enriched for inflammatory, immunosuppressive and immunoregulatory genes, while PF-B was enriched for anti-viral and adaptive-immune response genes [32], the latter likely contributing to a higher CTL infiltrate despite their low TMB, and better outcome in PF-B [31]. The pro-inflammatory IL6/STAT3 pathway plays a major role in driving tumorigenesis in PF-A ependymomas and contributes to proliferation, invasion and an immunosuppressive microenvironment mediated by tumor-associated myeloid cells [33], and the T-lymphocytes in PF-A show functional impairments in cytokine release [32]. Thus, targeting the IL6/STAT3 pathway has been suggested as potential strategy to reverse the immunosuppressive microenvironment in PF-A EPNs [33]. We did observe two PF-A EPNs expressing PD-L1, albeit in a very focal fashion (1–5% of tumor cells), in contrast to previous studies that have reported complete lack of PD-L1 IHC staining in PF EPNs. Witt et al. tested only 4 PF EPNs, Nam et al. tested 77 PF EPNs on tissue microarray sections with possibility of sampling bias, while Dumont et al. used a non-validated PD-L1 antibody clone [12, 14, 16]. Notably, both our PD-L1-positive PF-A tumors also harboured relatively higher CTLs with a positive correlation between PD-L1 staining and CTL density. Thus, while a minority of PF-A may be in a state of PD-L1-mediated immune escape, the majority lack significant CTL infiltrates and PD-L1 expression, and are unlikely candidates for ICB.

Previous two studies on EPNs reported lack of any prognostic value of PD-L1 in EPNs [15, 16]. In our cohort, patients with PD-L1-positive primary intracranial EPNs experienced longer median progression-free survival as compared to PD-L1-negative cases, although the differences did not reach statistical significance. We also noted

that recurrent EPNs less frequently expressed PD-L1. This weak positive prognostic association observed in primary EPNs, that nonetheless needs confirmation in larger patient cohorts enriched for ST-RELA tumors, is in stark contrast to the poor prognosis consistently described in PD-L1-positive glioblastomas [35]. Considering that primary EPNs with increased tumor infiltrating CTLs were also associated with longer PFS in our cohort as well as in previous published EPN cohorts [16, 31], the observed prognostic benefit of PD-L1 supports the premise that EPNs with an activated immune system are better able to curb tumor progression, as has been seen in advanced gastric cancers [36]. Thus, means to augment and manipulate such anti-tumor immune responses by ICB or other emerging immunotherapy modalities should be investigated and must be an area of focus in any research aimed at therapeutic targeting of ST-RELA EPNs.

Conclusion

Using PD-L1 and CD8 IHC, we found that PD-L1 expression correlates with increasing cytotoxic T-lymphocyte infiltrates in intracranial ependymomas. The majority of PD-L1-positive intracranial EPNs belong to the ST-RELA subset which also harbour the highest CTL densities. Our findings suggest that ST-RELA EPNs are potential candidates for immunotherapy targeting immune checkpoint modulators.

Author contributions NA: conceptualization, methodology, formal analysis, data curation, writing—original draft, and writing—review and editing; MPB: methodology, data curation, formal analysis, writing—review and editing; SA: data curation, writing—review and editing; BM: data curation, writing—review and editing; SM: data curation, writing—review and editing; SV: data curation, writing—review and editing; SC: data curation, writing—review and editing; SMC: conceptualization, methodology, funding acquisition, project administration, formal analysis, data curation, writing—original draft, and writing—review and editing

Funding This work is supported by the Science and Engineering Research Board (SERB) (EMR/2016/003365), New Delhi, India; Central Institute of Industrial research (CSIR), New Delhi, India (Pool No 8948A/17); and Neurosciences centre, AIIMS, New Delhi (intramural grants).

Compliance with ethical standards

Conflict of interest All authors declare no conflicts of interest.

Ethical approval The research has been ethically approved by the institute ethics committee (Ref. No. IEC-602/03.11.2017)

References

1. Ellison DW, McLendon R, Wiestler OD et al (2016) Ependymoma. In: Louis DN, Ohgaki H, Wiestler OD, Cavenee WK (eds) WHO classification of tumours of the central nervous system, 4th edn. IARC, Lyon, pp 106–112
2. Pajtler KW, Mack SC, Ramaswamy V, Smith CA, Witt H, Smith A et al (2017) The current consensus on the clinical management of intracranial ependymoma and its distinct molecular variants. Acta Neuropathol 133:5–12
3. Pajtler KW, Witt H, Sill M, Jones DT, Hovestadt V, Kratochwil F et al (2015) Molecular classification of ependymal tumors across all CNS compartments, histopathological grades, and age groups. Cancer Cell 27:728–743
4. Parker M, Mohankumar KM, Punchihewa C, Weinlich R, Dalton JD, Li Y et al (2014) C11orf95–RELA fusions drive oncogenic NF-κB signalling in ependymoma. Nature 506:451–455
5. Mack SC, Witt H, Piro RM, Gu L, Zuyderduyn S, Stütz AM et al (2014) Epigenomic alterations define lethal CIMP-positive ependymomas of infancy. Nature 506:445–450
6. Malgulwar PB, Nambirajan A, Pathak P, Faruq M, Rajeshwari M, Singh M et al (2018) C11orf95-RELA fusions and upregulated NF-KB signalling characterise a subset of aggressive supratentorial ependymomas that express L1CAM and nestin. J Neurooncol 138:29–39
7. Gessi M, Giagnacovo M, Modena P, Elefante G, Gianno F, Buttarelli FR et al (2019) Role of immunohistochemistry in the identification of supratentorial C11ORF95-RELA fused ependymoma in routine neuropathology. Am J Surg Pathol 43:56–63
8. Panwalkar P, Clark J, Ramaswamy V, Hawes D, Yang F, Dunham C et al (2017) Immunohistochemical analysis of H3K27me3 demonstrates global reduction in group-A childhood posterior fossa ependymoma and is a powerful predictor of outcome. Acta Neuropathol 134:705–714
9. Topalian SL, Hodi FS, Brahmer JR, Gettinger SN, Smith DC, McDermott DF et al (2012) Safety, activity, and immune correlates of anti-PD-1 antibody in cancer. N Engl J Med 366:2443–2454
10. Preusser M, Lim M, Hafler DA, Reardon DA, Sampson JH (2015) Prospects of immune checkpoint modulators in the treatment of glioblastoma. Nat Rev Neurol. 11:504–514
11. Kong LY, Wei J, Haider AS, Liebelt BD, Ling X, Conrad CA et al (2014) Therapeutic targets in subependymoma. J Neuroimmunol 277:168–175
12. Dumont B, Forest F, Dal Col P, Karpathiou G, Stephan JL, Vassal F et al (2017) PD1 and PD-L1 in ependymoma might not be therapeutic targets. Clin Neuropathol 36:90–92
13. Garber ST, Hashimoto Y, Weathers SP, Xiu J, Gatalica Z, Verhaak RG et al (2016) Immune checkpoint blockade as a potential therapeutic target: surveying CNS malignancies. Neuro Oncol 18:1357–1366
14. Witt DA, Donson AM, Amani V, Moreira DC, Sanford B, Hoffman LM et al (2018) Specific expression of PD-L1 in RELA-fusion supratentorial ependymoma: implications for PD-1-targeted therapy. Pediatr Blood Cancer 65:e26960
15. Hwang K, Koh EJ, Choi EJ, Kang TH, Han JH, Choe G et al (2018) PD-1/PD-L1 and immune-related gene expression pattern in pediatric malignant brain tumors: clinical correlation with survival data in Korean population. J Neurooncol 139:281–291
16. Nam SJ, Kim YH, Park JE, Ra YS, Khang SK, Cho YH et al (2019) Tumor-infiltrating immune cell subpopulations and programmed death ligand 1 (PD-L1) expression associated with clinicopathological and prognostic parameters in ependymoma. Cancer Immunol Immunother 68:305–318

17. Büttner R, Gosney JR, Skov BG, Adam J, Motoi N, Bloom KJ et al (2017) Programmed death-ligand 1 immunohistochemistry testing: a review of analytical assays and clinical implementation in non-small-cell lung cancer. J Clin Oncol 35:3867–3876
18. Cui S, Dong L, Qian J, Ye L, Jiang L (2018) Classifying non-small cell lung cancer by status of programmed cell death ligand 1 and tumor-infiltrating lymphocytes on tumor cells. J Cancer 9:129–134
19. Gandini S, Massi D, Mandalà M (2016) PD-L1 expression in cancer patients receiving anti PD-1/PD-L1 antibodies: a systematic review and meta-analysis. Crit Rev Oncol Hematol 100:88–98
20. Groot JFD, Penas-Prado M, Mandel JJ, O'Brien BJ, Weathers SPS, Zhou S et al (2018) Window of opportunity clinical trial of a PD-1 inhibitor in patients with recurrent glioblastoma. J Clin Oncol 36:2008. https://doi.org/10.1200/JCO.2018.36.15_suppl.2008
21. Spranger S, Spaapen RM, Zha Y, Williams J, Meng Y, Ha TT et al (2013) Up-regulation of PD-L1, IDO, and T(regs) in the melanoma tumor microenvironment is driven by CD8(+) T cells. Sci Transl Med 5:200ra116
22. Campesato LF, Barroso-Sousa R, Jimenez L, Correa BR, Sabbaga J, Hoff PM et al (2015) Comprehensive cancer-gene panels can be used to estimate mutational load and predict clinical benefit to PD-1 blockade in clinical practice. Oncotarget 6:34221–34227
23. Carbone M, Yang H, Gaudino G (2019) Does chromothripsis make mesothelioma an immunogenic cancer? J Thorac Oncol 14:157–159
24. Koirala P, Roth ME, Gill J, Piperdi S, Chinai JM, Geller DS et al (2016) Immune infiltration and PD-L1 expression in the tumor microenvironment are prognostic in osteosarcoma. Sci Rep 6:30093
25. Gorsi HS, Malicki DM, Barsan V, Tumblin M, Yeh-Nayre L, Milburn M et al (2019) Nivolumab in the treatment of recurrent or refractory pediatric brain tumors: a single institutional experience. J Pediatr Hematol Oncol 41:e235–e241
26. Mansfield AS, Peikert T, Smadbeck JB, Udell JBM, Garcia-Rivera E, Elsbernd L et al (2019) Neoantigenic potential of complex chromosomal rearrangements in mesothelioma. J Thorac Oncol 14:276–287
27. Gowrishankar K, Gunatilake D, Gallagher SJ, Tiffen J, Rizos H, Hersey P (2015) Inducible but not constitutive expression of PD-L1 in human melanoma cells is dependent on activation of NF-κB. PLoS One 10:e0123410
28. Fang W, Zhang J, Hong S, Zhan J, Chen N, Qin T et al (2014) EBV-driven LMP1 and IFN-γ up-regulate PD-L1 in nasopharyngeal carcinoma: implications for oncotargeted therapy. Oncotarget 5:12189–12202
29. Asgarova A, Asgarov K, Godet Y, Peixoto P, Nadaradjane A, Boyer-Guittaut M et al (2018) PD-L1 expression is regulated by both DNA methylation and NF-kB during EMT signaling in non-small cell lung carcinoma. Oncoimmunology 7:e1423170
30. Malgulwar PB, Nambirajan A, Pathak P, Rajeshwari M, Suri V, Sarkar C et al (2018) Epithelial-to-mesenchymal transition–related transcription factors are up-regulated in ependymomas and correlate with a poor prognosis. Hum Pathol 82:149–157
31. Donson AM, Birks DK, Barton VN, Wei Q, Kleinschmidt-Demasters BK, Handler MH et al (2009) Immune gene and cell enrichment is associated with a good prognosis in ependymoma. J Immunol 183:7428–7440
32. Hoffman LM, Donson AM, Nakachi I, Griesinger AM, Birks DK, Amani V et al (2014) Molecular sub-group-specific immunophenotypic changes are associated with outcome in recurrent posterior fossa ependymoma. Acta Neuropathol 127:731–745
33. Griesinger AM, Josephson RJ, Donson AM, Mulcahy Levy JM, Amani V, Birks DK et al (2015) Interleukin-6/STAT3 pathway signaling drives an inflammatory phenotype in Group A ependymoma. Cancer Immunol Res 3:1165–1174
34. Griesinger AM, Birks DK, Donson AM, Amani V, Hoffman LM, Waziri A et al (2013) Characterization of distinct immunophenotypes across pediatric brain tumor types. J Immunol 191:4880–4888
35. Xue S, Song G, Yu J (2017) The prognostic significance of PD-L1 expression in patients with glioma: a meta-analysis. Sci Rep 7:4231
36. Wang Y, Zhu C, Song W, Li J, Zhao G, Cao H (2018) PD-L1 expression and CD8(+) T cell infiltration predict a favorable prognosis in advanced gastric cancer. J Immunol Res 2018:4180517